Minimal Solutions to Generalized Three-View Relative Pose Problem
Supplementary Material

Yaqing Ding[1†], Chiang-Heng Chien[2†], Viktor Larsson[1], Karl Åström[1], Benjamin Kimia[2]
[1]Centre for Mathematical Sciences, Lund University
[2]School of Engineering, Brown University

1. Introduction

This supplementary material provides the following information: Section 2 describes the comparison between $\arccos$ and $\arcsin$ for computing the rotation and translation errors. Section 3 provides the experimental results using both intra- and inter-camera correspondences.

2. Comparison between $\arccos$ and $\arcsin$

To compute the relative rotation angle between two rotation matrices and relative angle between two translation vectors, we can use the $\arccos$ function given by

$$\xi_{\mathbf{R}_c} = \arccos\left(\frac{\mathrm{trace}(\mathbf{R}_{\mathrm{gt}}\mathbf{R}_{\mathrm{e}}^\top) - 1}{2}\right), \tag{1}$$

$$\xi_{\mathbf{t}_c} = \arccos\left(\frac{\mathbf{t}_g^\top \mathbf{t}_e}{\|\mathbf{t}_g\|\|\mathbf{t}_e\|}\right). \tag{2}$$

In this paper, we use the following $\arcsin$ formulation

$$\xi_{\mathbf{R}_s} = 2\arcsin\left(\frac{\|\mathbf{R}_{gt} - \mathbf{R}_e\|}{2\sqrt{2}}\right), \tag{3}$$

$$\xi_{\mathbf{t}_s} = 2\arcsin\left(\frac{1}{2}\left\|\frac{\mathbf{t}_e}{\|\mathbf{t}_e\|} - \frac{\mathbf{t}_g}{\|\mathbf{t}_g\|}\right\|\right). \tag{4}$$

To prove that they are mathematically equivalent and show the benefits of using $\arcsin$ over $\arccos$ for numerical precision, consider (3),

$$\begin{aligned}
\|\mathbf{R}_{gt} - \mathbf{R}_e\| &= \sqrt{\mathrm{trace}((\mathbf{R}_{gt} - \mathbf{R}_e)^\top(\mathbf{R}_{gt} - \mathbf{R}_e))} \\
&= \sqrt{\mathrm{trace}(2\mathbf{I} - \mathbf{R}_{gt}^\top\mathbf{R}_e - \mathbf{R}_e^\top\mathbf{R}_{gt})} \\
&= \sqrt{6 - 2\mathrm{trace}(\mathbf{R}_{gt}^\top\mathbf{R}_e)} \\
&= \sqrt{4 - 4\cos(\xi_{\mathbf{R}_c})} \\
&= \sqrt{8\sin^2(\frac{\xi_{\mathbf{R}_c}}{2})}.
\end{aligned} \tag{5}$$

† Equal contribution.

Comparing (3) with (5) we have $\xi_{\mathbf{R}_s} = \xi_{\mathbf{R}_c}$, *i.e.*, (1) is equivalent to (3).

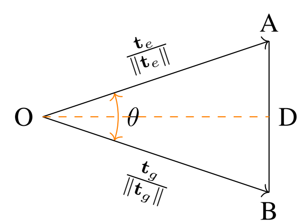

Figure 1. Using $\arcsin$ to compute the angle of two vectors.

The derivation of (4) is illustrated in Figure 1. Since $\overrightarrow{OA}$ and $\overrightarrow{OB}$ are normalized translation vectors, we have

$$\sin(\frac{\theta}{2}) = \frac{1}{2}\|\overrightarrow{OA} - \overrightarrow{OB}\| = \frac{1}{2}\left\|\frac{\mathbf{t}_e}{\|\mathbf{t}_e\|} - \frac{\mathbf{t}_g}{\|\mathbf{t}_g\|}\right\| \tag{6}$$

In this case, Eq. (4), which is mathematically equivalent to (2), can be obtained.

To illustrate the benefits of using $\arcsin$ formulations, we generate random rotation matrices and translation vectors as ground truth. Then we add small noise ($[10^{-15}, 10^{-12}]$) to the ground truth to simulate the estimations. Figure 2 shows the comparisons between $\arccos$ and $\arcsin$ for the rotation and translation error computation. It can be seen from the plots that $\arcsin$ performs significantly better than $\arccos$ when the estimation is close to the ground truth, *i.e.*, $\arcsin$ can demonstrate the numerical stability of solvers. $\arccos$ returns many zero values due to the precision limitations.

3. Results with inter correspondences

Due to the lack of space we only show the median results and CDF using intra correspondences in the paper, results for inter-camera correspondences and mean errors are shown in Figure 3 and Table 1. An illustration of the intra- and inter-camera correspondences is shown in Figure 4.

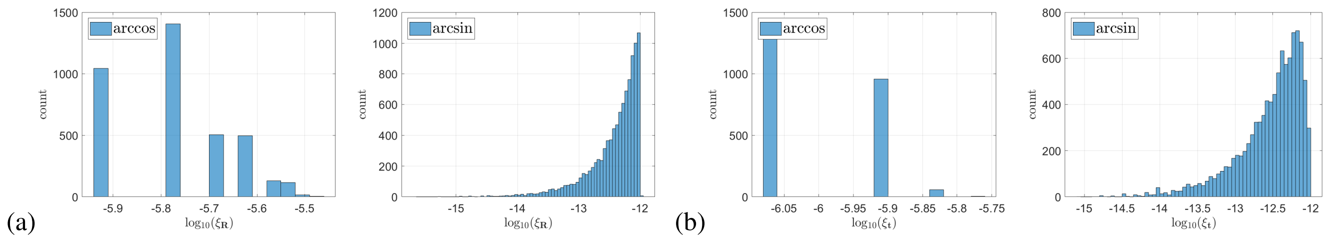

Figure 2. Comparison between arccos and arcsin. (a) Rotation error. (b) Translation error.

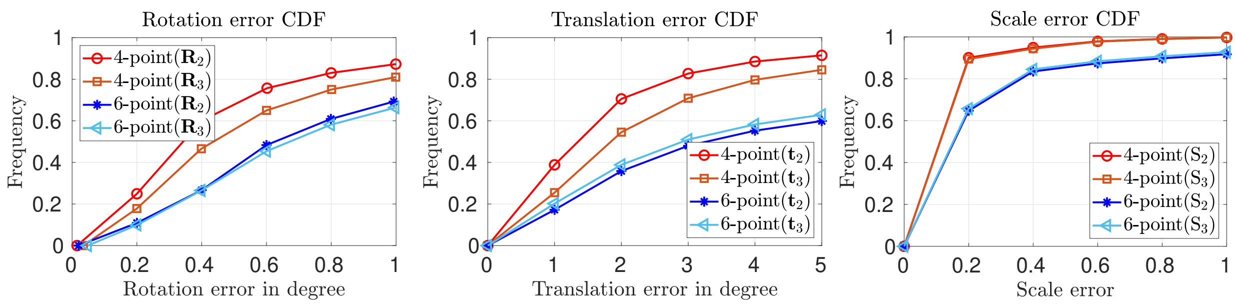

Figure 3. The cumulative distribution functions of the relative errors using both intra- and inter-camera correspondences for all the image pairs. Being accurate is interpreted as a curve close to the top-left corner.

LaMAR	Solver	$\xi_{\mathbf{R}}$	$\xi_{\mathbf{t}}$	ξ_{S}	Inlier	Iter
Median	4-point	0.37	1.51	0.04	946	100
	6-point	0.61	3.05	0.12	915	245
Mean	4-point	0.93	3.48	0.09	1494	99
	6-point	1.78	9.61	0.41	1458	257

Table 1. Results on the LaMAR dataset using both intra- and inter-camera correspondences.

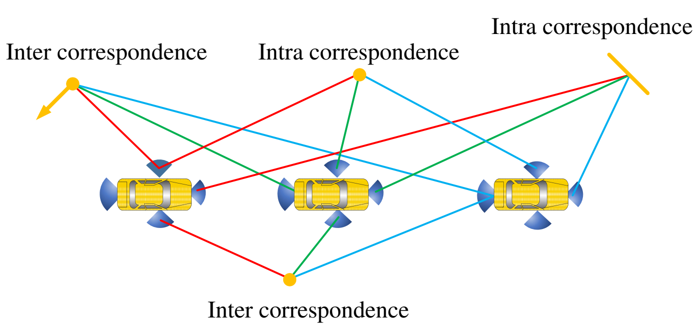

Figure 4. Illustration of intra- and inter-camera correspondences. Intra-camera correspondence: the feature is observed by the same camera of a multi-camera system. Intel-camera correspondence: the feature is observed by different cameras of a multi-camera system.